

1995

Failure modes and gradual degradation due to large electrical stresses in GaAs/AlGaAs heterojunction bipolar transistors

Michael D. Wetzel
Lehigh University

Follow this and additional works at: <http://preserve.lehigh.edu/etd>

Recommended Citation

Wetzel, Michael D., "Failure modes and gradual degradation due to large electrical stresses in GaAs/AlGaAs heterojunction bipolar transistors" (1995). *Theses and Dissertations*. Paper 387.

This Thesis is brought to you for free and open access by Lehigh Preserve. It has been accepted for inclusion in Theses and Dissertations by an authorized administrator of Lehigh Preserve. For more information, please contact preserve@lehigh.edu.

Wetzel,
Michael D.

Failure Modes
and Gradual
Degradation Due
to Large Electrical
Stresses in
GaAs/AlGaAs...

October 8, 1995

**FAILURE MODES AND GRADUAL DEGRADATION DUE TO
LARGE ELECTRICAL STRESSES IN GaAs/AlGaAs
HETEROJUNCTION BIPOLAR TRANSISTORS**

by

Michael D. Wetzel

A Thesis

Presented to the Graduate and Research Committee

of Lehigh University

in Candidacy for the Degree of

Master of Science

in

Electrical Engineering

Lehigh University

13 September 1995

This thesis is accepted and approved in partial fulfillment of the requirements for
the Master of Science in Electrical Engineering.

9/17/95

Date

Professor J. C. M. Hwang

Thesis Advisor

Professor A. McAulay

Chairman of Department

Acknowledgements

I would like to thank my advisor, Dr. James C. M. Hwang for his support, valuable suggestions, and guidance. My colleagues in the Compound Semiconductor Technology Laboratory—Mr. Hai-Chan Chung, in particular—have also been an enormous source of knowledge, insight, encouragement, and support.

I extend loving thanks to my parents, my brother, and my grandparents for their unwavering support of my studies and confidence in me. I would also like to thank my friends outside the lab who never let me forget to enjoy these precious years.

Table of Contents

List of Figures	v
Abstract	1
Chapter 1 Introduction	2
Chapter 2 Experiment	4
2.1 Format of Devices	4
2.2 Measurement Setup	5
2.3 Characterization	6
2.4 Stress	8
Chapter 3 Results of Stress	10
3.1 Open-Base Stress	10
3.2 Open-Collector Stress	13
3.3 Open-Emitter Stress	13
Chapter 4 Failure Modes	16
Chapter 5 Conclusions	19
Chapter 6 Future Work	21
References	22
Figures	23
Vita	33

List of Figures

- Figure 1. Cross section of a gallium arsenide/aluminum gallium arsenide heterojunction bipolar transistor
- Figure 2. Measurement setup
- Figure 3. dc iv characteristics of HBT #1 ($80 \mu\text{m}^2$)
- Figure 4. Forward Gummel plot for HBT #7 ($40 \mu\text{m}^2$)
- Figure 5. Reverse Gummel plot for HBT #7 ($40 \mu\text{m}^2$)
- Figure 6. Collector-emitter breakdown behavior of HBT #4 ($80 \mu\text{m}^2$)
- Figure 7. Collector-base breakdown behavior of HBT #9 ($30 \mu\text{m}^2$)
- Figure 8. dc iv characteristics of HBT #3 ($80 \mu\text{m}^2$), before and after stress
- Figure 9. Forward Gummel plot for HBT #3 ($80 \mu\text{m}^2$), before and after stress
- Figure 10. Evolution of collector-base breakdown current for HBT #9 ($30 \mu\text{m}^2$)

Abstract

The effects of different electrical (as opposed to thermal) stresses on gallium arsenide/aluminum gallium arsenide (GaAs/AlGaAs) heterojunction bipolar transistors (HBTs) has been studied. Three failure modes have been identified. They are instantaneous burn-out, long-term catastrophic burn-out, and gradual parametric degradation. Potential reasons that lead to each of the failure modes are discussed. Further, different types of electrical stress have been found to favor certain modes of failure over others. The practical implications of these findings is mentioned.

Chapter 1

Introduction

The heterojunction bipolar transistor (HBT) (see Figure 1 for basic device structure) has several inherent advantages over the conventional silicon (Si) bipolar junction transistor (BJT) [1]: A wide-band-gap emitter allows the use of a very heavily doped base with a lightly doped emitter, while maintaining high emitter injection efficiency with lower parasitic resistances and capacitances than for a conventional homojunction bipolar transistor. High electron mobility, built-in drift fields, and velocity overshoot combine to reduce electron transit time through the device. Semi-insulating substrates help reduce pad parasitics and allow convenient integration of devices.

Because of these advantages, HBTs are being increasingly used in integrated circuits where high speed and high frequency operation are required [1]. Some typical circuit applications of HBTs include high-efficiency microwave and millimeter-wave power amplifiers, oscillators, mixers, and analog-to-digital (A/D) and digital-to-analog (D/A) converters.

As the popularity of the HBT grows, however, its reliability becomes more of a concern. To date the GaAs/AlGaAs HBT reliability literature has concentrated on base-dopant outdiffusion and emitter-contact degradation under high collector currents [2]. In contrast, RF power Si BJT literature has concentrated on dc forward-current-gain (β) degradation under high collector voltages [3]. It appears that the Si/SiGe HBT has an

edge over the Si BJT in this area. Because the GaAs/AlGaAs HBT is often seen as a substitute for the Si-based devices it is important to know where its performance falls.

This paper investigates failure modes of GaAs/AlGaAs HBTs when subjected to large electrical stresses. The possible failure modes are instantaneous burn-out, long-term catastrophic burn-out, and gradual parametric degradation. Which failure mode dominates depends on the fabrication technology and the operating conditions. Gradual parametric degradation is the most interesting of these modes and is the focus of this study.

Chapter 2

Experiment

Several HBT samples were electrically stressed on a microwave probe station. In referring to specific devices, an arbitrary numbering system (#1, #2, and so on) has been used. The format of the devices tested is first described in Section 2.1. The setup used to measure and stress the devices is then examined in Section 2.2. Section 2.3 contains the details on the measurements made to characterize the devices, while Section 2.4 contains information on how the devices were stressed.

2.1 Format of Devices

HBT samples were supplied by an outside company. The samples were on wafer segments or chips. Each chip's total surface area was divided into three regions. Two of the regions each contained one amplifier. The last region was devoted to a process control monitor (PCM).

This PCM contained several test patterns for checking continuity, measuring resistances and the like, and also several discrete devices. The work has focused on three particular devices. One of the devices was RF-probable, and the other two were dc-probable.

The RF-probable device is referred to as such because it was designed with ground-signal-ground (GSG) probe contacts on both the input and output sides. The pitch of the pads (the distance from the center of one pad to the center of an adjacent pad) was

175 μm . The device was designed in a common-emitter configuration with the emitter via-hole grounded.

The dc-probable devices had pads which allowed access to each of the device's terminals. None of the terminals was tied to ground.

The RF-probable device had 2 emitter fingers each measuring 2 μm wide by 20 μm long for a total emitter area of 80 μm^2 . The dc-probable devices each had only one emitter finger measuring 10 μm long. For one of the devices, the finger was 3 μm wide, giving a total emitter area of 30 μm^2 . For the other, it was 4 μm wide, giving an area of 40 μm^2 .

Each of the supplied chips was attached to an electrically- and thermally-conductive piece of copper which served as a chip carrier. Attachment was made with a silver epoxy to ensure good electrical contact between the chip carrier and the backside of the chip. This is important as the RF-probable devices are grounded through via-holes. If the emitters of these devices are forced to float electrically, oscillations may prevent clean device operation.

2.2 Measurement Setup

The physical setup used in probing, characterizing, and stressing the devices is illustrated in Figure 2. The setup is built around a commercially available microwave probe station from Rucker & Kolls (Model 250). The chip carrier is positioned on the stage of the probe station. The probe positioners have magnetic bases which allow them to be easily fixed into place on the platform of the probe station. In the case of the RF-probable device, a pair of coaxial RF probes from GGB Industries (Model #40A-GSG-

175-EDP) are used to make contact. In the case of the dc-probable device, a pair of dc "needle" probes from Alessi are used to make contact. A microscope allows visual inspection of the devices and probes. A fiber optic illuminator provides additional light to improve the quality of the image seen through the microscope.

2.3 Characterization

The HBTs are first dc characterized to establish some performance benchmarks prior to any stressing. In all, four types of dc measurements are made on each device. These measurements are repeated at certain time intervals during the stress to track any degradation.

First, the iv characteristic curves are measured. The collector current (I_C) is measured as a function of collector-emitter voltage (V_{CE}) for several base currents (I_B). A typical set of curves is shown in Figure 3 for HBT #1. This device is an $80 \mu\text{m}^2$ device. Thermal effects can be seen for base injections greater than about 1 mA.

Both the forward and reverse Gummel plots are also measured. In the forward Gummel plot the base and collector currents are measured as a function of base-emitter bias for the case of the base-collector junction shorted. The base-emitter bias is swept from the region where the diode is essentially off, through turn-on, and into saturation. The currents are plotted on a logarithmic scale. From the Gummel plot it is easy to determine values for the forward-current-gain (β) in the different regions of base-emitter bias. β is one of the parameters monitored to gauge gradual degradation. Changes in β for certain ranges of junction bias can provide information about what is happening at a device junction as the device is degrading. Reverse Gummel plots are essentially the

same as forward plots—the only difference being that the roles of the collector and emitter are reversed for the measurement. Figure 4 shows the forward Gummel plot for HBT #7. Figure 5 shows the reverse Gummel plot for HBT #7.

The last dc measurement performed on the HBTs is one of the reverse breakdown behavior. From this can be determined both a breakdown voltage—some BV —and also a stressing condition. The type of breakdown measurement made is determined by the type of stress that is to be done. As will be seen in Chapter 3 the devices have been subjected to three different types of dc stress: 1.) open-base stress, 2.) open-collector stress, and 3.) open-emitter stress. In the first case, knowledge of collector-emitter breakdown is important. In the second, emitter-base breakdown, and in the third, base-collector breakdown. The first and third cases are actually quite similar. A large collector-emitter bias applied with the base open tends to set up some small base-emitter forward bias with the rest of the voltage falling across the base-collector, thereby reverse-biasing that junction. Figures 6 and 7 show some typical breakdown characteristics. Note the extreme negative differential resistance regions in Figure 6.

The iv characteristics and the Gummel plots are measured with a Hewlett-Packard 4142B Modular dc Source/Monitor (Figure 2). This instrument is capable of supplying voltages (with current compliances) and currents (with voltage compliances) and measuring resulting voltages and currents. It is controlled by an IBM-compatible personal computer and communication between the two is via the General Purpose Interface Bus (GPIB), IEEE Standard 488. An HP-EEsof software product ANACAT

[4] allows users to write programs in a pseudo-BASIC language that instruct the 4142 to make the desired measurements. The raw measurement data is stored in ASCII files.

The breakdown studies are done manually with a Hewlett-Packard 6644A System dc Power Supply (Figure 2). While it is of course possible to perform this measurement with the 4142 as well, it is not recommended because the 4142 may not respond to the current compliance quick enough to prevent the device from burning. The breakdown current is after all exponentially dependent upon the reverse-bias voltage. So small changes in applied voltage lead to large changes in resulting current. And the measurement with the 6644A is not any more difficult. It just takes a bit longer, and the data must be entered into the computer by hand.

2.4 Stress

The goal of this work is to see device degradation resulting from hot electron-hole pairs created in the high electric field region of the HBT—not from the current/thermal effects mentioned in Chapter 1. So it is important to select a stress condition that will maximize the electrical stress on the device while minimizing device heating. This is accomplished by reverse-biasing one of the junctions and leaving the other terminal open, as mentioned in Section 2.3.

The reverse-biased junction is usually biased either at or into breakdown. With the HBTs that are the subject of this study, the breakdown mechanism is avalanche breakdown. Once the breakdown behavior of a device has been measured (as described in Section 2.3), a stress voltage can be chosen. That voltage is then applied between the terminals corresponding to the stress that is to be done.

The dc stress is applied for some time interval over which the resulting breakdown current is monitored. A Hewlett-Packard 34401A Multimeter has been used to make the periodic measurements. It is remotely-controlled by an IBM-compatible personal computer with communication via GPIB. The control program has been written in TransEra's TBASIC [5] programming language. The measurement data is written to ASCII files as in the iv and Gummel plot measurements discussed in Section 2.3.

The stress is then removed and the first three of the dc characterization measurements are performed. It is not necessary to repeat the breakdown measurement. Any parametric changes are noted and stressing is resumed. The point at which it can be conclusively said that there has been some device degradation is when one parameter has changed by 10%. It is typical to look for a 10% decrease in β . One item that is still not clear is whether or not some observable change in the breakdown current monitored during the stress is a precondition for degradation.

Chapter 3

Results of Stress

In all, a total of eleven HBTs have been stressed. Six of them were stressed in the open-base configuration. One was stressed in the open-collector configuration. The remaining four were stressed in the open-emitter configuration.

3.1 Open-Base Stress

As stated above, the first six samples (#1-#6) were stressed in the open-base configuration. The stress voltage was applied collector to emitter with the emitter grounded. All of these devices were of the RF-probable variety where the emitter pads were via-hole grounded to the stage of the probe station. The negative terminal of the power supply was tied to ground and those grounds were connected together.

The first sample, HBT #1, was step-stressed with increasing V_{CE} . In between stress voltages, the dc iv curves were measured. Forward-current-gain, β , was chosen as the parameter to monitor to determine whether or not any gradual parametric degradation was taking place. β values were just computed from the iv curves, as β is just the base injection divided by the collector current at some collector-emitter voltage where the device is turned on.

$$\beta = \frac{I_B}{I_C}$$

At a collector-emitter voltage of 11.6 V the device suddenly burned. The current that corresponded to that voltage was 10 mA. The dc power dissipated by the device can be computed from the product of the voltage applied across the device and the current through it:

$$\begin{aligned}P_{dc} &= I_{CE} \times V_{CE} \\ &= (10 \text{ mA}) \times (11.6 \text{ V})\end{aligned}$$

$$P_{dc} = 116 \text{ mW}.$$

The power density can be computed by dividing this value by the effective junction area:

$$P_{dens} = \frac{P_{dc}}{A_{junc_eff}}$$

In the case of this stress, the area is just the base-emitter junction area. So for this $80 \mu\text{m}^2$ device, we have a power density of $(116 \times 10^{-3} \text{ W}) / (80 \times 10^{-8} \text{ cm}^2) = 1.45 \times 10^5 \text{ W/cm}^2$. This power density is on the order of the thermal limit of typical power HBTs [1]. β remained constant at about 29 throughout the stress.

The initial dc characteristics of HBT #2 were very similar to those of HBT #1, with the exception of the measured collector-emitter breakdown characteristic. Above $V_{CE} = 10 \text{ V}$, the breakdown current increased far more rapidly than it did for HBT #1. When the device was stressed in this region it burned almost immediately. The stress point was $V_{CE} = 10.1 \text{ V}$ and $I_{CE} = 14 \text{ mA}$. The dc power would then be 141.4 mW, and the power density $(141.4 \times 10^{-3} \text{ W}) / (80 \times 10^{-8} \text{ cm}^2) = 1.77 \times 10^5 \text{ W/cm}^2$. This is also on the order of the thermal limit.

The breakdown behavior of HBT #3 more closely resembled that of HBT #1, but did exhibit a negative differential resistance which was also seen in HBT #2. β of HBT #3, however, was 10% lower (26 vs. 29) than either HBT #1 or HBT #2 right from the start. HBT #3 was stressed with collector-emitter voltages that ranged from 10.4 to 12.3 V, corresponding to a collector current range of 1 to 10 mA. No change in HBT characteristics was observed until about 7 mA. With a 7 mA or higher stress, β decreased by approximately 0.1 after 1 h (Fig. 8). Figure 9 shows quite clearly that there is also a decrease in the base leakage current before the base-emitter junction is turned on—effectively *increasing* β in this region. Under a collector current stress of 10 mA, the collector voltage of HBT #3 quickly increased beyond 13 V and then dropped to 3 V, resulting in permanently distorted dc characteristics.

HBTs #4 and #5 exhibited notably different collector-emitter breakdown behaviors than any of the previous devices. The breakdown currents measured for each reverse-breakdown voltage were lower than those seen for the first three devices. HBT #4 and #5 did behave very much like each other though. Both devices burned at roughly the same dc power level. HBT #4 burned at an applied collector-emitter voltage of 12 V. The measured breakdown current at this voltage was 7.5 mA. The power then comes to 90 mW, and the power density to 1.13×10^5 W/cm². HBT #5 burned at the same collector-emitter voltage, but at a current of 7.6 mA. The power here is 91.2 mW, and the power density is 1.14×10^5 W/cm². Once again, we observe burn-out at power densities at the thermal limit.

The final device stressed in this configuration was HBT #6. This device burned in the same manner as all of the aforementioned devices, but did so at a decidedly lower power density— $5.55 \times 10^4 \text{ W/cm}^2$ —which is about half of the value typically used to mark the thermal limit, $1 \times 10^5 \text{ W/cm}^2$. $V_{CE} = 11.1 \text{ V}$ and $I_{CE} = 4 \text{ mA}$.

3.2 Open-Collector Stress

One of the samples (#7) was stressed in the open-collector configuration. This device was one of the dc-probable devices. None of the terminals were tied to any particular reference by the manufacturer; all of the terminals could be freely manipulated by the tester. The stress voltage was applied between the base and the emitter. The emitter was connected to the positive terminal of the power supply and the base was connected to the negative terminal of the power supply with that terminal tied to ground.

HBT #7 accepted reverse-breakdown voltages well past BV_{EBO} —which was measured to be 8.8 V—without any appreciable change in dc characteristics. Once the applied voltage reached 9.4 V, however, the device burned. The breakdown current that was measured at this point was approximately 3 mA. The corresponding dc power was then 28.2 mW. Calculating the power density for this $40 \mu\text{m}^2$ device we see that it is $7.05 \times 10^4 \text{ W/cm}^2$. Again this is approaching the thermal limit.

3.3 Open-Emitter Stress

The last four samples (#8-#11) were stressed in the open-emitter configuration. As with the device discussed in Section 3.2, all of these devices were of the dc-probable variety. The stress voltage was applied between the base and the collector. The

collector was connected to the + terminal of the power supply and the base was connected to the - terminal of the power supply with that terminal tied to ground.

HBT #8 burnt out instantaneously at $V_{CE} = 21$ V and $I_{CB} = 6.55$ mA. That corresponds to a dc power of about 138 mW. Using the method of calculating the power density described and used in the previous two sections, we find a power density of approximately 4.6×10^5 W/cm² for this 30 μm^2 device. This is well above the thermal limit of 1×10^5 W/cm² previously established under open-base and open-collector conditions. The device should have burnt out long before reaching this point. It can be concluded that, under open-emitter stresses, the breakdown and burn-out involve mainly the extrinsic base-collector junction which has an area much larger than the intrinsic base-collector junction area. This conclusion is supported by the fact that, given the geometry of an HBT (see Fig. 1), breakdown current between the collector and base will largely flow from the collector contact through the extrinsic part of the base-collector junction to the base contact. The symmetry of the device and the open emitter prevent much current from flowing through the intrinsic part of the junction.

Under open-emitter conditions, the base-collector reverse-breakdown characteristic for HBT #9, a 30 μm^2 device, is illustrated in Figure 7. Using the manufacturer's criterion of 4 $\mu\text{A}/\mu\text{m}^2$ or 4×10^2 A/cm², the open-emitter base-collector reverse-breakdown voltage, BV_{CBO} , is approximately 17 V. This breakdown current increases to approximately 2×10^3 A/cm² at 18 V. Since this is where the current really starts to turn up, this was decided on to be the next stressing voltage.

The remaining three HBTs (#9, #10, and #11) were each stressed at a reverse base-collector voltage of 18 V and exhibited long-term catastrophic burn-out after 1.4, 1.1, and 2.6 h, respectively. Prior to burn-out, the reverse base-collector current gradually degraded up to a few percents (about 5%) as shown in Figure 10 for HBT #9.

Chapter 4

Failure Modes

It can be readily seen from the results detailed in Chapter 3 that there are three distinct failure modes that have manifested themselves in the electrical stressing of GaAs/AlGaAs HBTs. They are 1.) instantaneous burn-out, 2.) long-term catastrophic burn-out, and 3.) gradual parametric degradation.

The first failure mode, instantaneous burn-out, was the most common mode encountered in this study. It was found to be the cause of failure in the majority of the devices stressed in the open-base configuration. It was also the cause of failure in the one device that was stressed in the open-collector configuration. This failure mode basically results when the device is exposed to too much power. In other words, when the device is required to dissipate more power than it is capable of. The device is overwhelmed immediately and burns. The failure mode is truly a thermally-driven degradation mechanism that results from an electrical stress.

The second failure mode, long-term catastrophic burn-out, is also a thermally-driven mechanism, but it differs from the instantaneous burn-out in that it occurs over some finite amount of time. The device is not initially overwhelmed with power, but over time the heating builds. Eventually a critical point is reached and the device burns. This kind of failure could be seen in the last three HBTs. The devices could endure the stress for an hour or two, but after that, they would burn.

The last failure mode observed degraded the device in some measurable way over time. That is, from the onset of stress some degradation takes place. This is in contrast with the second mode of failure—which builds over time—but affects the device all at once—completely destroying it. The degradation is seen by measuring some of the benchmark quantities that people use to rate devices, the most common one for bipolar devices being the forward-current-gain β .

This failure mode is clearly the mode at work in HBT #3. Changes in β have been observed in both the forward-active region of operation as well as in the region where the base-emitter junction is just coming on. In the forward-active region, β was observed to have decreased by about 1%. In the region where the base-emitter junction is just coming on, β was observed to have increased by about 50%.

It is believed that this failure mode is also at work in HBTs #9, #10, and #11. It can be seen that the breakdown current flowing in HBT #9 is increasing—albeit slightly—with stress time. If the stress condition was relaxed a bit, degradation over a longer period of time might be possible without the catastrophic burn-out at the end.

It is interesting to theorize about what is the fundamental mechanism that gives rise to this last failure mode. Clearly, this mode is electrically-driven as opposed to thermally-driven. It is believed that when the junctions of the HBT are reversed-biased far enough into breakdown the electric field at the junctions can be so large that carriers moving through the field become so energized that they can create additional electron-hole pairs through impact ionization [6]. Where these newly-created carriers end up is not always clear. They could somehow end up being injected into the passivation of the

device creating traps at the passivation-semiconductor interface, thereby disturbing the flow of charge and degrading device performance.

Chapter 5

Conclusions

Different failure modes that result from electrical stress of the junctions in a gallium arsenide/aluminum gallium arsenide heterojunction bipolar transistor have been studied.

Instantaneous burn-out is the most likely mode of failure when the power density exceeds the thermal limit. This is typically thought of as around 1×10^5 W/cm².

Long-term catastrophic burn-out is observed when power densities are on the order of about one order of magnitude below the thermal limit. The cases that demonstrated long-term catastrophic burn-out in this study sustained power densities of $(18 \text{ V})(0.6 \times 10^{-3} \text{ A})/(30 \times 10^{-8} \text{ cm}^2) = 3.6 \times 10^4$ W/cm², or $(18 \text{ V})(0.6 \times 10^{-3} \text{ A})/(40 \times 10^{-8} \text{ cm}^2) = 2.7 \times 10^4$ W/cm², for periods of about an hour or two.

Gradual parametric degradation is the most interesting, but was also the most difficult to come by. When it does occur, the easiest and most important parameter to watch is the forward-current-gain β . A change in β on the order of 1% was observed in this study.

The type of degradation that can be expected varies with the type of stress done. The open-base and open-collector stress configurations are dominated by instantaneous burn-out failures. The open-collector stress reverse-biases and stresses the base-emitter junction. The open-base stress reverse-biases and stresses the intrinsic part of the base-

collector junction. The area of each of these regions is much smaller than the area of the extrinsic base-collector junction. This extrinsic base-collector junction is the region that dominates in an open-emitter stress. The sheer size of this region keeps the power density in the device during the stress low. This allows the device to experience a true electrical stress and degrade gradually long before reaching the thermal limit. So even though the most conclusive parametric degradation was observed with a device that was stressed open-base (HBT #3), the open-emitter configuration offers the best chance to see gradual degradation.

The practical implication of knowing which kind of stress will gradually degrade an HBT is that it becomes much easier to study this particular failure mode. More study will hopefully lead to a better understanding of the fundamental mechanism that gives rise to gradual parametric degradation. Any solution that could be found would be of particular interest to people involved with pulsed operation under Class B or C conditions of a radar transmitter.

Chapter 6

Future Work

More work should be done to experimentally verify that open-emitter stressing will in fact provide a better means for examining gradual parametric degradation of HBTs than open-base stressing.

As gradual parametric degradation can now more easily be studied, an investigation into the fundamental mechanism that is responsible for it should be done.

RF stressing might provide valuable insight into this problem. It would also give people in the industry a more immediate feeling for what kinds of problems they can expect with their devices and circuits.

References

- [1] F. Ali and A. Gupta (Eds.), *HEMTs & HBTs: Devices, Fabrication, and Circuits*, Artech House, Inc., 1991.
- [2] S. Tanaka, H. Shimawaki, K. Kasahara, and K. Honjo, "Characterization of current-induced degradation in Be-doped HBTs based in GaAs and InP," *IEEE Transactions on Electron Devices*, July 1993, pp. 1194-1201.
- [3] D. R. Sparks, "Hot carrier degradation in polyemitter NPN transistors from BVebo, BVceo, BVeco and BVcbo stress conditions," *Proceedings of the Symposia on Reliability of Semiconductor Devices/Interconnections and Dielectric Breakdown for Microelectronic Applications*, 1992, pp. 205-215.
- [4] HP-EEsof, Inc., Westlake Village, CA.
- [5] TransEra Corp., Provo, UT.
- [6] R. Muller and T. Kamins, *Device Electronics for Integrated Circuits, Second Edition*, John Wiley & Sons, Inc., 1986, pp. 193-198.

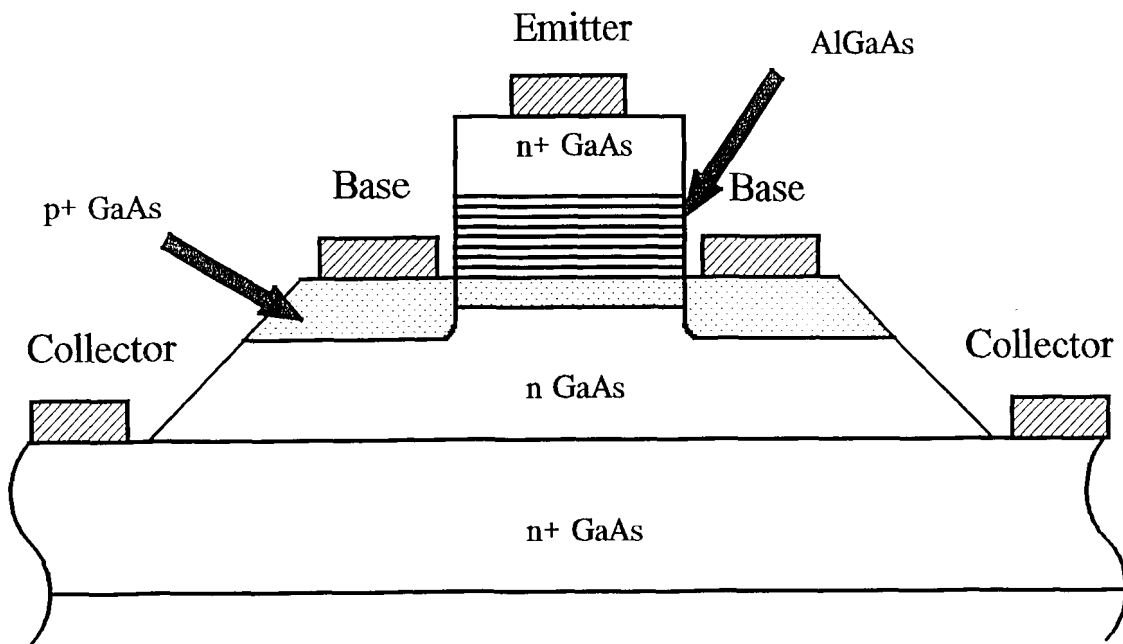


Figure 1. Cross section of a gallium arsenide/aluminum gallium arsenide heterojunction bipolar transistor

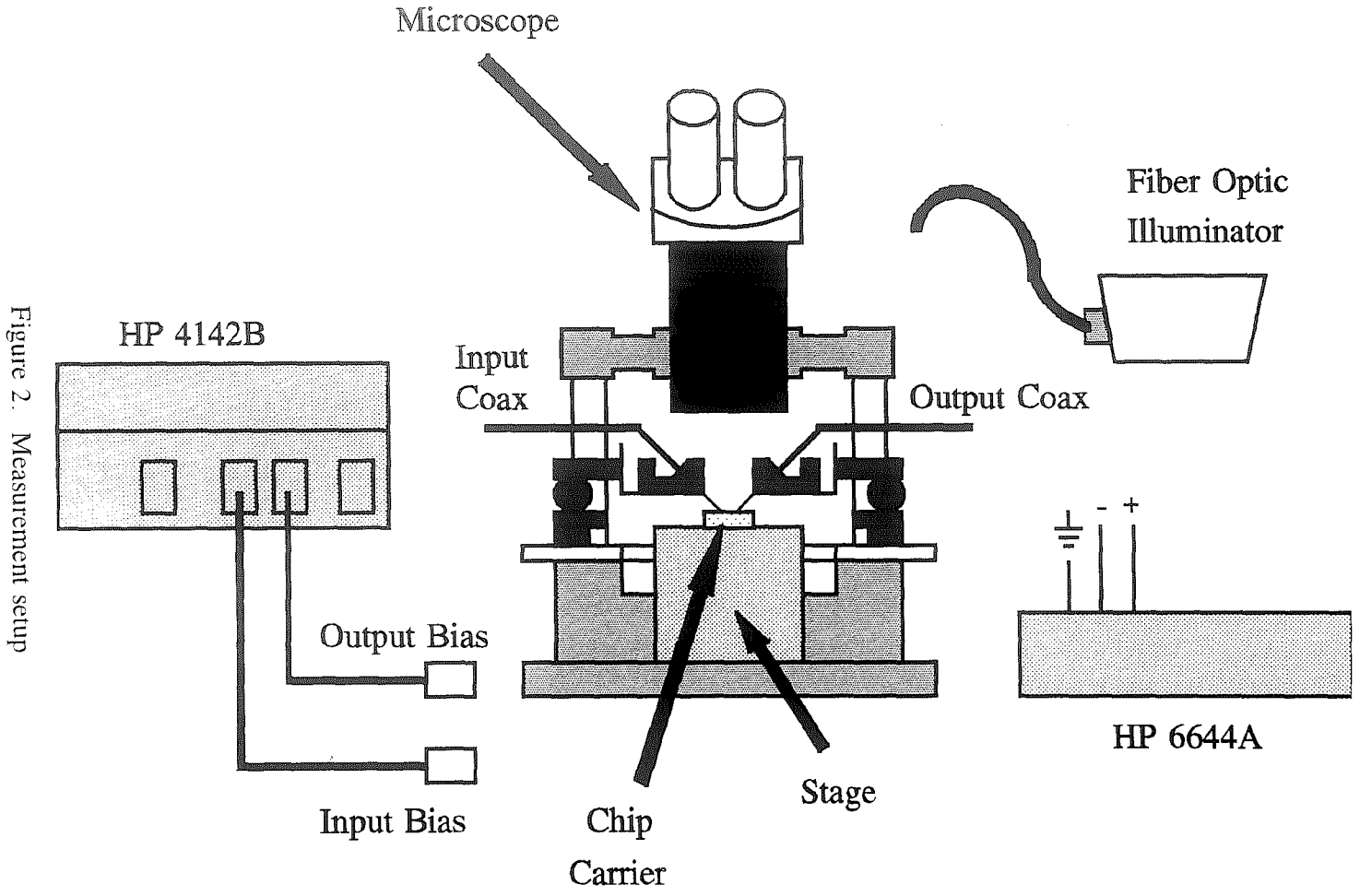


Figure 2. Measurement setup

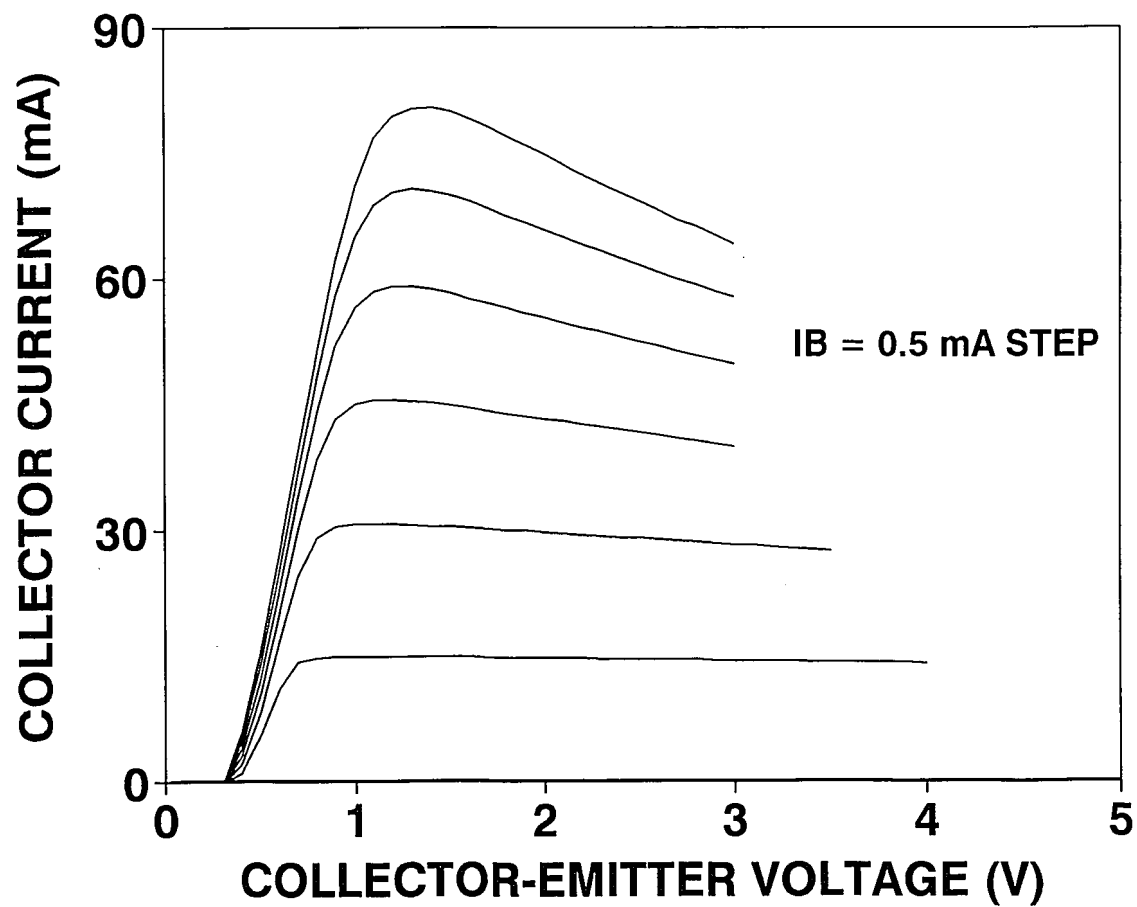


Figure 3. dc iv characteristics of HBT #1 (80 μm^2)

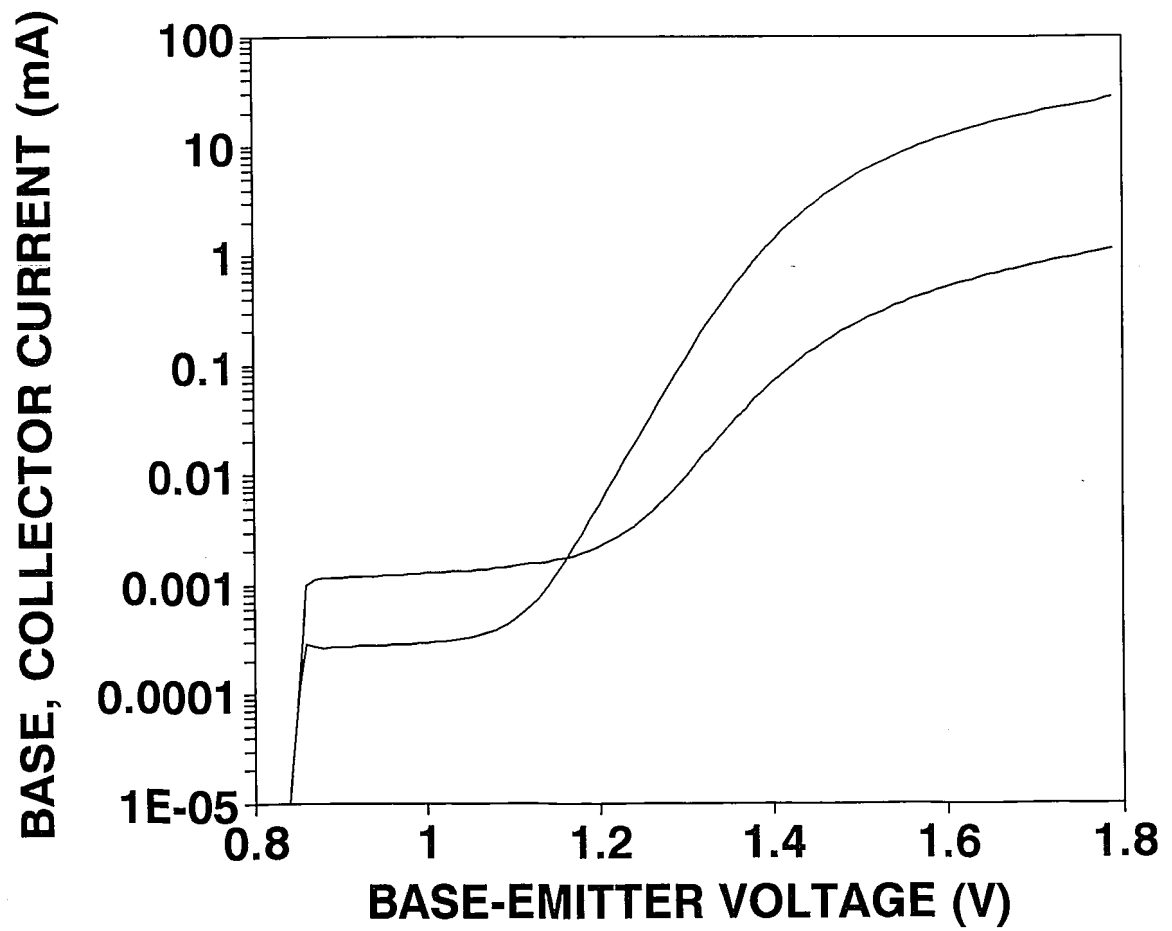


Figure 4. Forward Gummel plot for HBT #7 ($40 \mu\text{m}^2$)

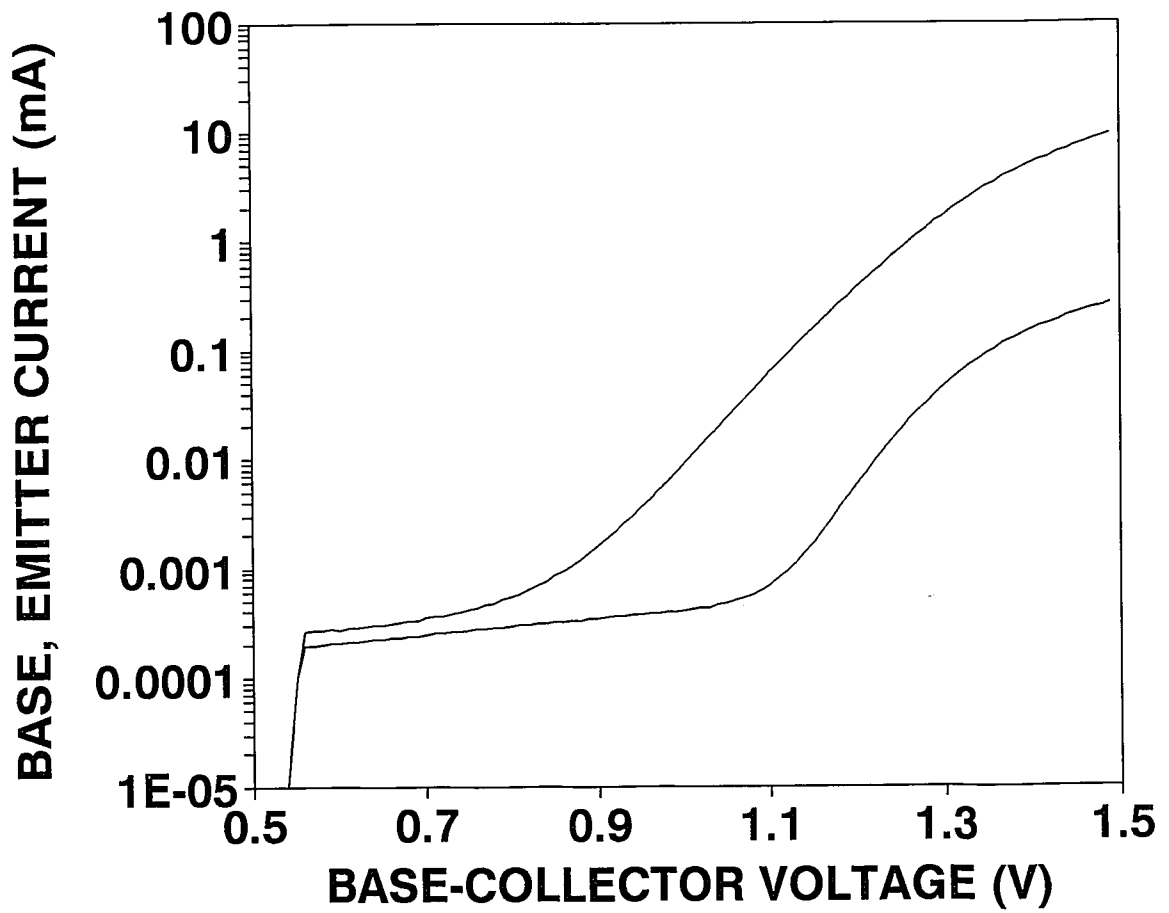


Figure 5. Reverse Gummel plot for HBT #7 (40 μm²)

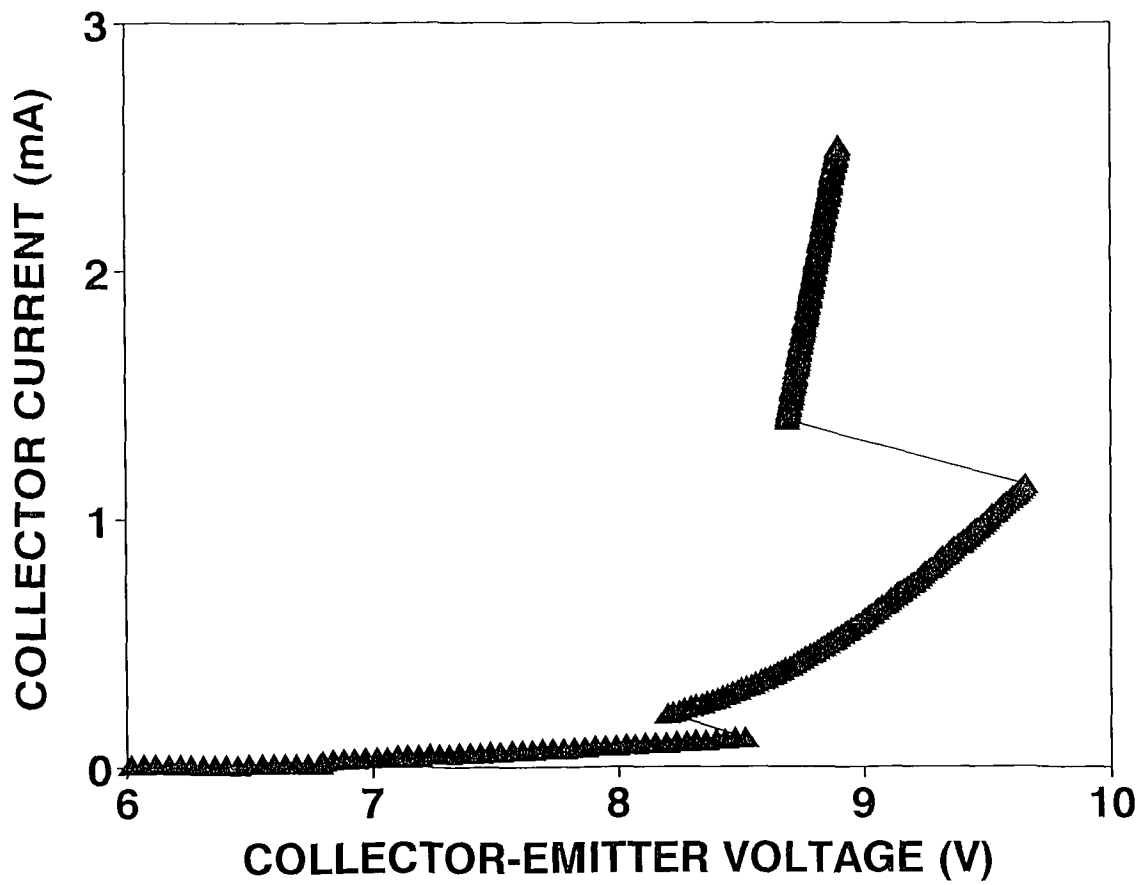


Figure 6. Collector-emitter breakdown behavior of HBT #4 ($80 \mu\text{m}^2$)

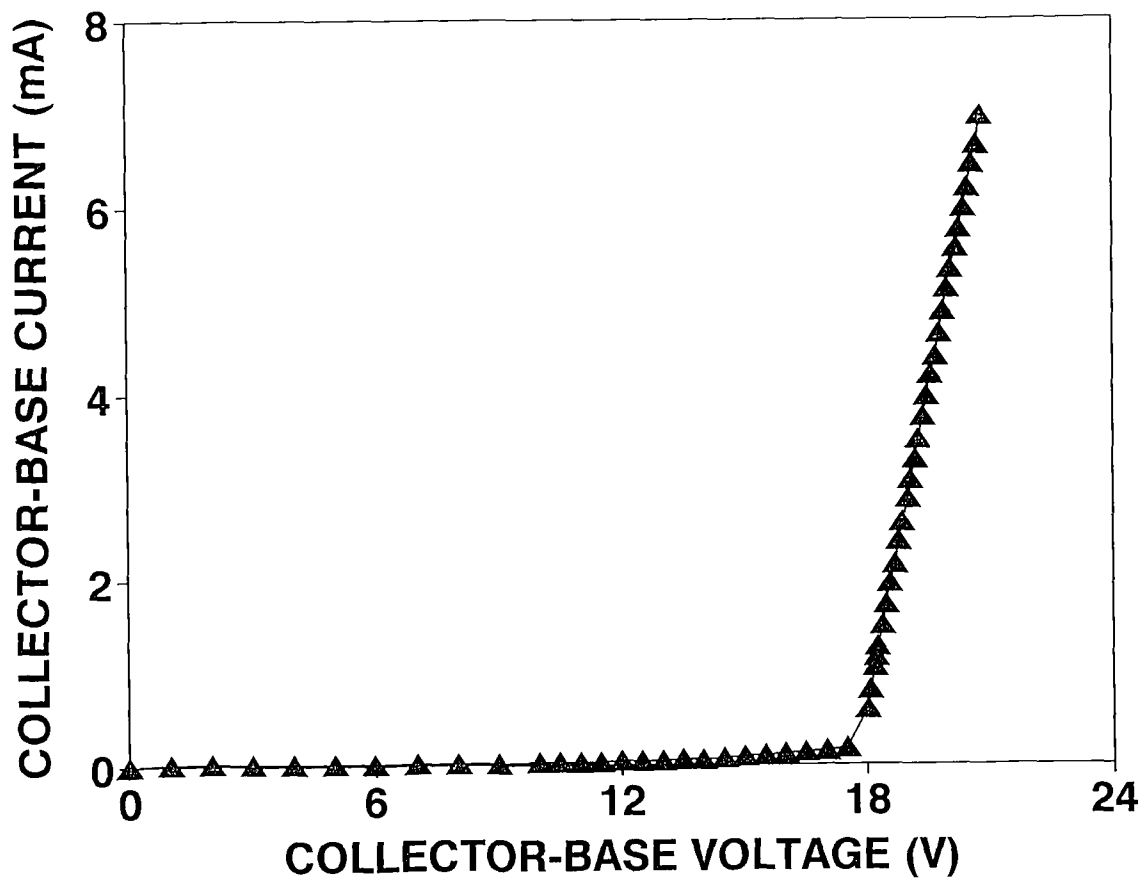


Figure 7. Collector-base breakdown behavior of HBT #9 ($30 \mu\text{m}^2$)

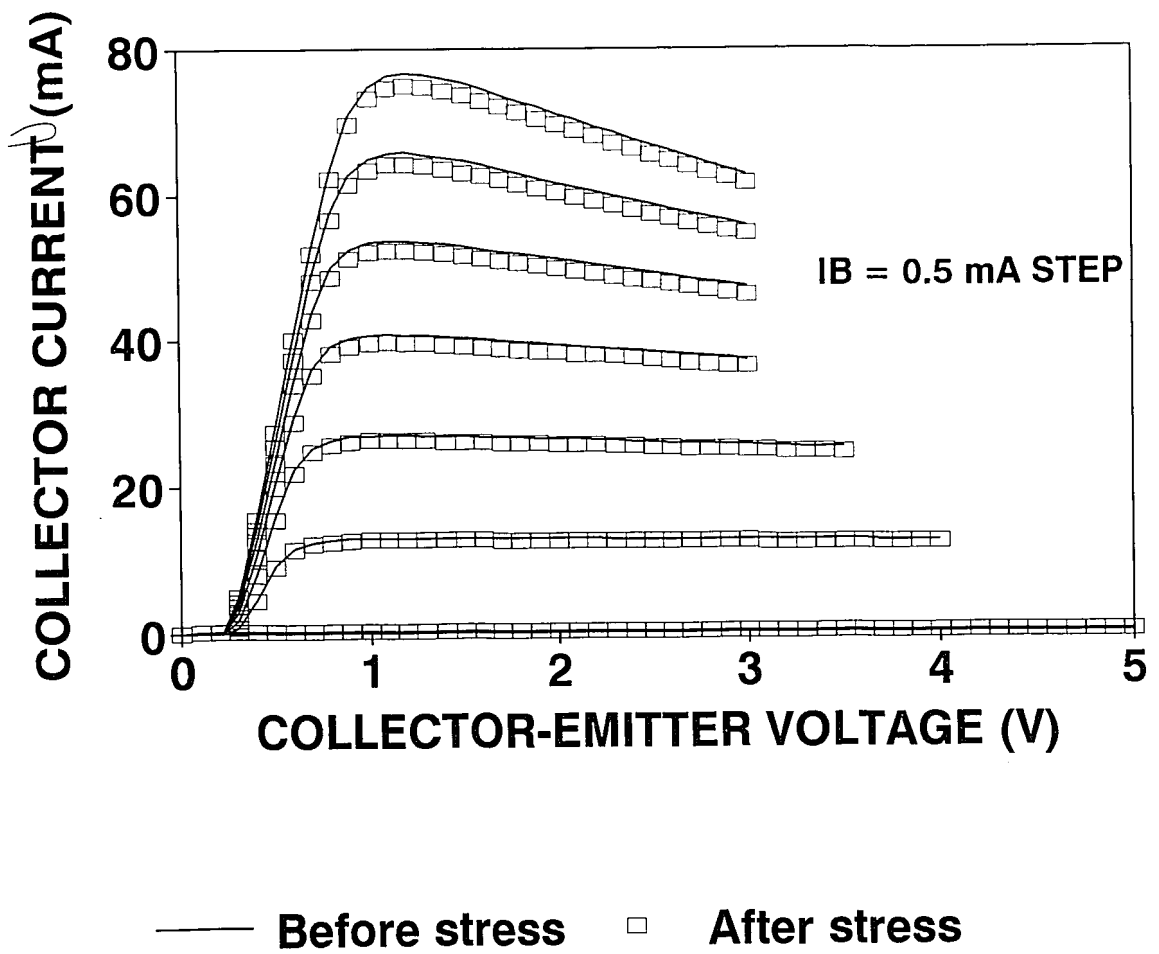


Figure 8. dc iv characteristics of HBT #3 ($80 \mu\text{m}^2$), before and after stress

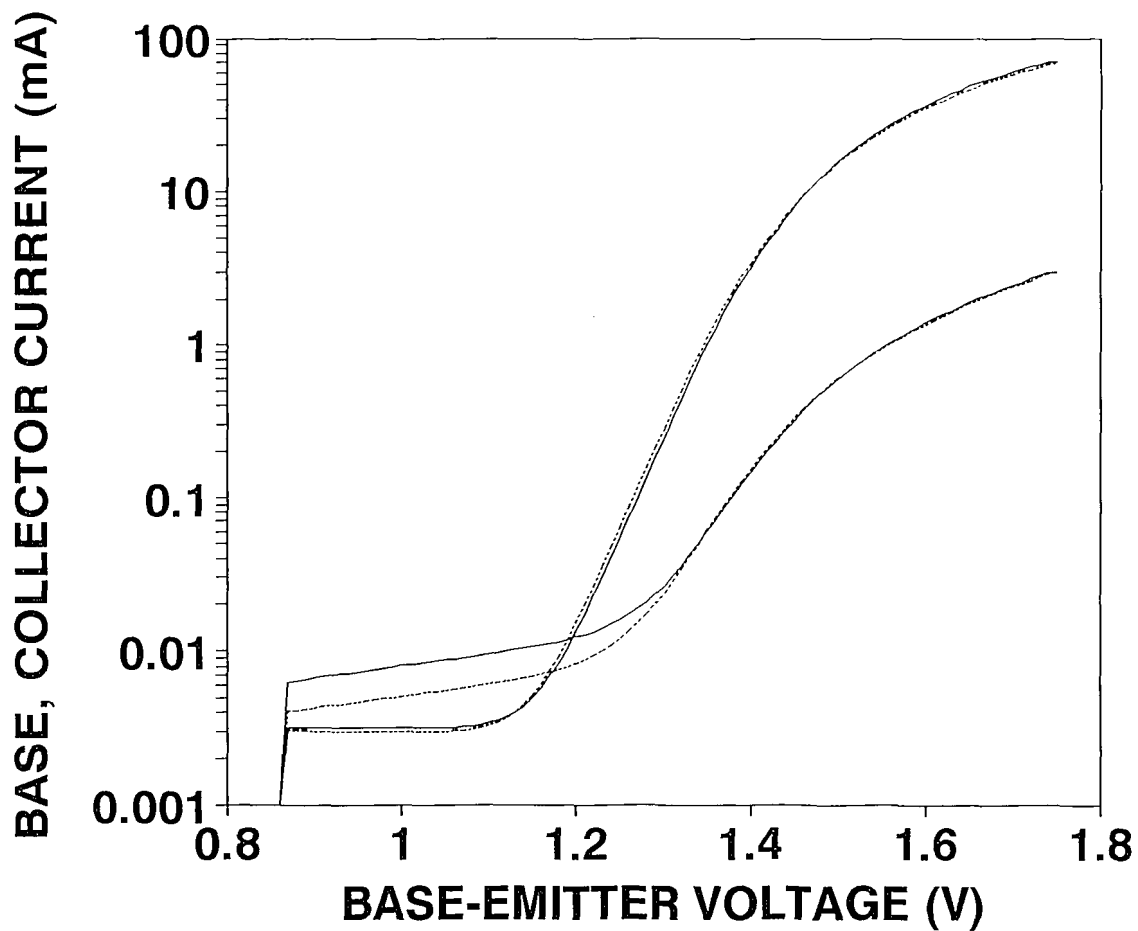


Figure 9. Forward Gummel plot for HBT #3 ($80 \mu\text{m}^2$), before and after stress

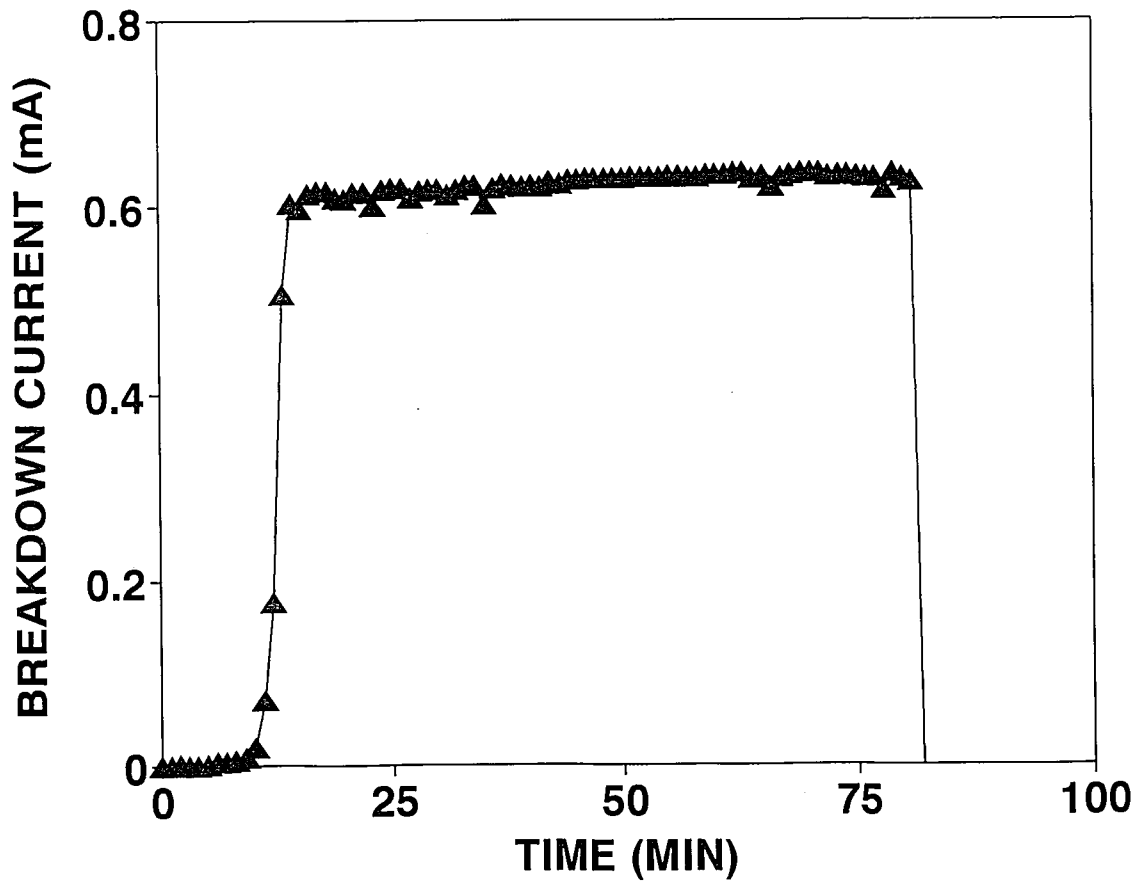


Figure 10. Evolution of collector-base breakdown current for HBT #9 ($30 \mu\text{m}^2$)

Vita

Michael D. Wetzel was born in Allentown Pennsylvania on 13 November 1970. He obtained Bachelor of Science degrees in both Electrical Engineering and Engineering Physics from Lehigh University by May 1993. In the Fall of 1993 he began his graduate studies at Lehigh University. He has worked on microwave device characterization and reliability testing in the Compound Semiconductor Technology Laboratory.

**END
OF
TITLE**